16

Process Design for Economic, Environmental and Safety Objectives with an Application to the Cumene Process

Shivom Sharma, Zi Chao Lim and Gade Pandu Rangaiah
Department of Chemical and Biomolecular Engineering,
National University of Singapore, Singapore

16.1 Introduction

In process design, performance objectives such as costs and safety often conflict. Multi-objective optimization (MOO) improves decision making by providing many optimal (non-dominated) solutions for understanding quantitative tradeoffs and for selection of a suitable optimal solution. The non-dominated solutions obtained are equally good mathematically for the given objectives. One or more of them can be chosen preferentially over others for implementation, based on other requirements and preference. Besides the optimal values of the objectives, the corresponding values of decision variables are of interest in the selection and implementation of one of the optimal solutions. Hence, the use of MOO is important for the design and operation of industrial processes. Performance criteria such as capital cost, profit, net present worth, and energy have been used for the optimization of industrial processes. Many of these criteria are related to the economic performance of the process. In recent times, non-economic performance criteria such as environmental impact and the safety of a process have been becoming increasingly important. Hence, it is desirable to

Multi-Objective Optimization in Chemical Engineering: Developments and Applications, First Edition.
Edited by Gade Pandu Rangaiah and Adrián Bonilla-Petriciolet.

consider safety and environmental objectives along with economic objectives in process design with MOO.

Emissions from the process affect the environment. Life-cycle assessment, the methodology of environmental impact minimization, waste reduction algorithm, and environmental fate and risk assessment tools are commonly used for the evaluation of environmental impact of processes (Ramzan and Witt, 2006). Several indicators (e.g., human toxicity potential and global warming potential) quantify environmental impacts in different categories. These indicators are aggregated to quantify the combined impact of a chemical process on the environment (e.g., potential environmental index—PEI). In several MOO studies, chemical processes are simultaneously optimized for economic and environmental objectives; for example, Hoffmann *et al.* (2004) explored design alternatives for HCN production, Guillen-Gosalbez *et al.* (2007) optimized hydrodealkylation of toluene to benzene, Gebreslassie *et al.* (2009) optimized an absorption-cooling system, and Lee and Rangaiah (2009) optimized VOC (i.e., volatile organic compounds) recovery and solvent recovery processes.

Recently, Sharma *et al.* (2011) investigated four environmental criteria, namely, PEI, IMPact Assessment of Chemical Toxics 2002+ (IMPACT), green degree (GD) and inherent environmental toxicity hazard (IETH) for optimization of both VOC and solvent recovery processes. IMPACT calculations are easier than others, and the use of aggregate IMPACT is similar to the use of its individual categories. Sometimes, emitted chemicals are burnt for their fuel value, but ultimately they enter and affect the environment in the form of carbon dioxide. Hence, minimization of emissions of chemicals from a process reduces its adverse environmental impact as well as leading to better utilization of raw materials. Further, emissions from a process can be calculated very quickly using process simulation results compared to aggregated indicators, which require suitable databases.

Several methodologies have been developed to identify the hazard and risk involved in processes. These include hazard and operability studies (HAZOP), occupational safety and health assessment series (OSHAS 18000 and 18001, n.d.), and failure mode and effects analysis (FMEA). Hazard-identification methodologies and tools identify different problems, which arise after operation failure (Khan *et al.*, 2001). Further, safety measures such as control and protective systems can only be used at the end of process design. Moreover, hazard identification and mitigation require high-quality technical expertise and substantial monetary and time investments throughout plant life (Khan and Amyotte, 2005).

On the other hand, process design considering inherent safety is relatively safer at lower capital and operating costs (Khan and Amyotte, 2005). Ultimately, this approach reduces the intrinsic hazard potential of the process. Further, high production capacity increases the hazard potential of a plant (Khan and Amyotte, 2004). Process safety indices for possible use at the preliminary design stage are reviewed in the next section. Some of them have been employed in process optimization. For example, the Dow Fire and Explosion Index (Dow F&EI), with some modification, was used to quantify the inherent safety of a process (Suardin *et al.*, 2007); the modified Dow F&EI was then used as a safety indicator along with an economic objective in the design and optimization of a reaction-separation system. Shah *et al.* (2009) have analyzed the inherent safety of a propane pre-cooled gas-phase liquefied natural-gas process based on liquid hydrocarbon inventory. Recently, Li *et al.* (2011) used an enhanced Inherent Safety Index to quantify the safety of a bio-diesel process.

In this chapter, the Integrated Inherent Safety Index (I2SI) of Khan and Amyotte (2004) is selected as the process safety objective, material loss from the process is used to quantify the environmental burden, and total capital cost (TCC) is chosen as an economic objective for MOO of the cumene process at the preliminary design stage. For this, the cumene process is simulated using Aspen Hysys v-7.2, and it is then optimized for economic, environmental and safety (EES) objectives simultaneously using the elitist non-dominated sorting genetic algorithm (NSGA-II). Three bi-objective and one tri-objective optimization problems are studied. The Pareto-optimal fronts obtained from the MOO of the cumene process are presented and discussed, both in objective and decision variable space. These results give better insights into tradeoffs among EES objectives and for the selection of a suitable process design.

The next section of this chapter reviews selected safety indices in the literature, and discusses I2SI in detail. Section 16.3 describes cumene process, its simulation and costing. Section 16.4 presents an I2SI calculation for the cumene process. Section 16.5 describes the MOO program used for cumene process optimization. Sections 16.6 and 16.7 present and discuss the optimization results for bi- and tri-objective optimization problems, respectively. Useful conclusions and insights from this work are given at the end of this chapter.

16.2 Review and Calculation of Safety Indices

Safety considerations include risk of potential damage to process equipment, workers and people in the plant's vicinity. Several indices have been proposed to quantify process safety. The Dow F&EI has been used to quantify fire and explosion potential of a process; it requires historical loss data, energy potential of different materials, and the extent to which loss prevention practices are applied in the process (Kidam *et al.*, 2008). Dow F&EI cannot be used for determining safety in the conceptual design and preliminary process development stages (Lees, 2005). The Dow CEI (Chemical Exposure Index) determines the relative safeness of a process under specific process conditions, in terms of toxicity (Khan *et al.*, 2003). The Mond Index (Khan and Abbasi, 1998) is a hazard-assessment index similar to the Dow F&EI, with additional hazard considerations.

The Prototype Index of Inherent Safety (PIIS) of Edwards and Lawrence (1993) includes inherent safety related to chemical reactions, while the Inherent Safety Index (ISI) of Heikkilä *et al.* (1996) considers the inherent safety of both reaction and separation steps. The ISI is categorized into two subgroups: the chemical inherent safety index and the process safety index. The i-Safe index (Palaniappan *et al.*, 2004) combines subindices from the PIIS and ISI. Recently, Al-Sharrah *et al.* (2007) proposed the K index, which assesses process safety using the probability of an incident and the magnitude of the resulting damage; it cannot analyze the effects of operating conditions, and also requires historical data. Srinivasan and Kraslawski (2006) applied the TRIZ (theory of inventive problem solving) creativity enhancement approach to design inherently safer chemical processes. Srinivasan and Nhan (2008) proposed an Inherent Benign-ness Indicator (IBI), which is based on principal component analysis (PCA), for comparing inherent safety of various process routes. Banimostafa *et al.* (2012) further evaluated the potential of the PCA-based method for process route selection.

Hazard Identification and Ranking System (HIRA) of Khan and Abbasi (1998) combines the FEDI (Fire and Exposure Damage Index) and the TDI (Toxic Damage Index). For FEDI calculation, various process units are classified into five categories: storage, physical operation, chemical reaction, transportation and other hazardous units (e.g., furnaces, boilers and direct-fired heat exchangers). In each category, energy factors are calculated based on the physical and chemical properties, state of material and operating conditions. Subsequently, penalties accounting for operating conditions, chemical properties, plant capacity and surrounding parameters are estimated (Khan and Abassi, 1998). The TDI represents the lethal toxic load over an area, measured in terms of radius of area (in meters), with 50% probability of causing fatality. In this, penalties are similar to those assigned for FEDI, with additional consideration for chemical toxicity and dispersion of released chemicals. Many of the penalties used for calculating FEDI and TDI are derived using models from thermodynamics, transport phenomena, heat transfer, and fluid dynamics. A few penalties are quantified using empirical models and hazard ranking procedures. The Safety Weighted Hazard Index (SWeHI; Khan *et al.*, 2001) improves the HIRA by including safety measures required to minimize potential hazards, assessing adequacy of existing control systems, and site-specific attributes. Later, Khan and Amyotte (2004) developed I2SI, which identifies potential hazards throughout the life cycle of a process/plant. It comprises two main indices: the Hazard Index (HI) and the Inherent Safety Potential Index (ISPI).

16.2.1 Integrated Inherent Safety Index (I2SI)

The I2SI is a comprehensive safety index that considers a wide range of potential hazards, and allows process designers to investigate the effects of process conditions. Apart from hazard identification, it can also be applied in route selection and rapid risk assessment. As shown in Figure 16.1, the I2SI calculation requires the Damage Index (DI), Process and Hazard Control Index (PHCI) and Inherent Safety Index (ISI). The DI, PHCI, ISI and hence I2SI are calculated for each process unit. Finally, the I2SI for the entire process is obtained by summing I2SI of each and every unit in the process.

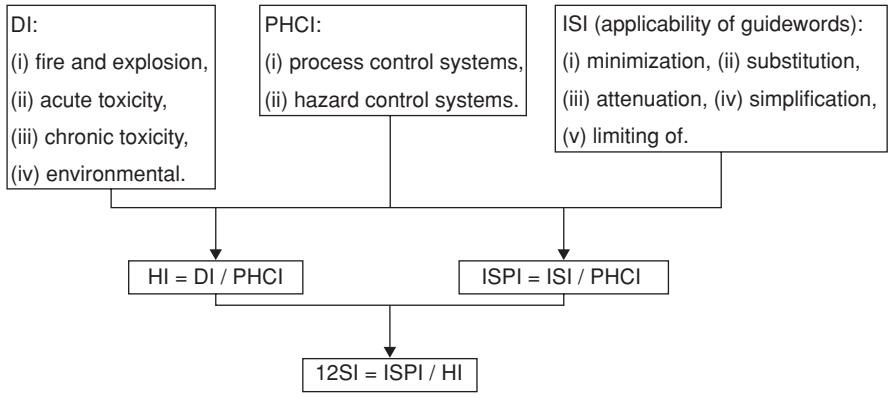

Figure 16.1 *Flowchart for I2SI calculation for each process unit (Khan and Amyotte, 2004); DI—Damage Index; PHCI—Process and Hazard Control Index; ISI—Inherent Safety Index; HI—Hazard Index; ISPI—Inherent Safety Potential Index.*

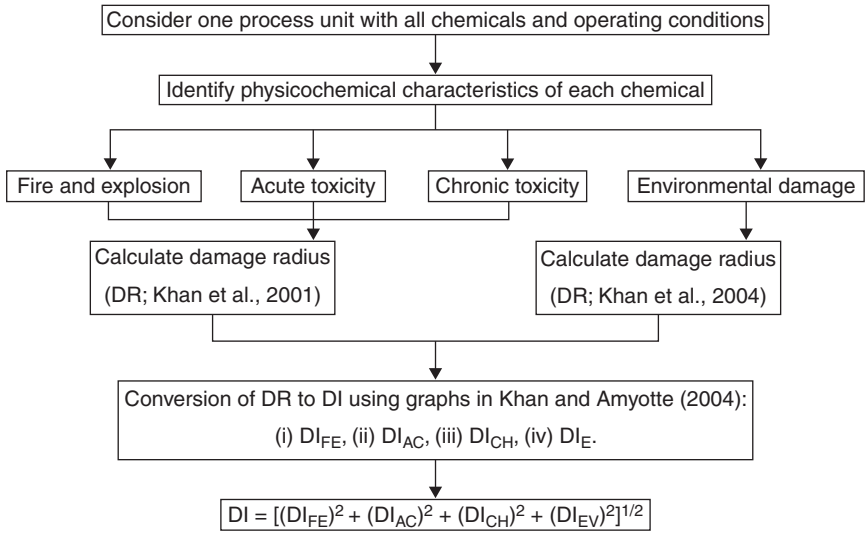

Figure 16.2 *Flowchart for DI calculation for each process unit (Khan and Amyotte, 2004); DR—damage radius; DI—Damage Index; DI_{FE}—Fire and Explosion Damage Index; DI_{AC}—Acute Toxicity Damage Index; DI_{CH}—Chronic Toxicity Damage Index; DI_{EV}—Environmental Damage Index.*

Figure 16.2 presents a flowchart for DI calculation for each process unit. Four types of hazards, namely, fire and explosion, acute toxicity, chronic toxicity, and environmental damage are considered in the DI calculation. In Figure 16.2, damage radii (DR) for fire and explosion (FEDR) and acute/chronic toxic release (TDR) are calculated using the SWeHI approach. A detailed flowchart for the DR calculation is given in Figure 16.3. It mainly involves: (i) quantification of core/energy factors according to process unit type, (ii) assignment of penalties, and (iii) estimation of DR based on core factors and penalties. The FEDR and TDR are converted to the respective DI using graphs in Khan and Amyotte (2004). The DI calculation for environmental damage is adapted from Khan *et al.* (2004); it considers impact of chemicals on air, water and soil. These chemicals are further classified according to the National Fire Protection Association (NFPA) ranking. Monographs in Khan and Amyotte (2004) are used to convert environmental DR to DI.

Figure 16.4 presents a flowchart for PHCI calculation for each unit. The PHCI assesses various process-control and hazard-control measures that are required or present in the process (Khan and Amyotte, 2004). The abscissa value in the range of 1 to 10 is assigned to each process-control and hazard-control system/measure. The PHCI of the respective control system can be determined using figures in Khan and Amyotte (2004). Then, the PHCI for an i^{th} process unit can be obtained by adding PHCI values for all control systems used in that process unit.

$$\mathrm{PHCI_i} = \sum_{\mathrm{j}} \mathrm{PHCI_j} \tag{16.1}$$

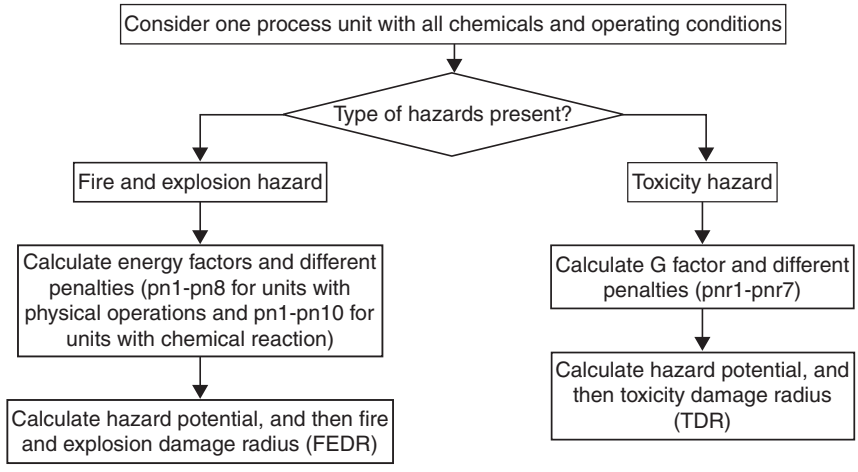

Figure 16.3 *Flowchart for DR calculation using the Safety Weighted Hazard Index (SWeHI) approach for each process unit (Khan* et al.*, 2001); see Appendices A and B for penalty calculations.*

Here, the summation is over all process control and hazard control systems in the i^{th} process unit.

The evaluation of ISI requires the application of guidewords similar to HAZOP studies. For each process unit, the index value of each guideword is estimated based on the extent of guideword applicability, and using figures and tables in Khan and Amyotte (2004). For a process unit, final ISI value for a process unit is obtained by combining ISI value for all guidewords. Figure 16.5 presents a flowchart including the final equation for the ISI calculation.

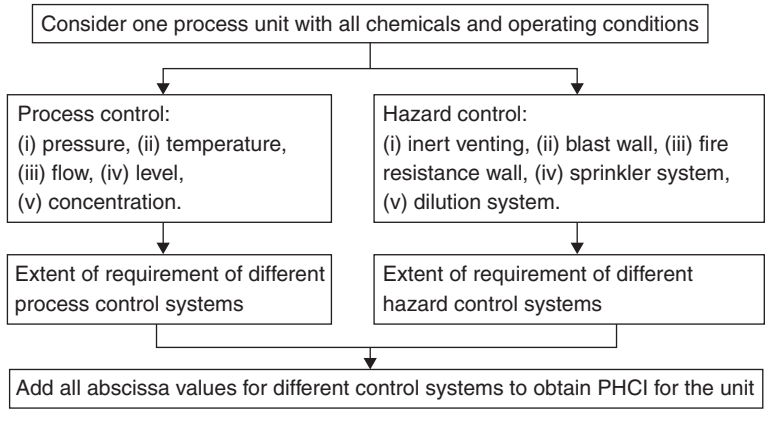

Figure 16.4 *Flowchart for PHCI calculation for each process unit (Khan and Amyotte, 2004).*

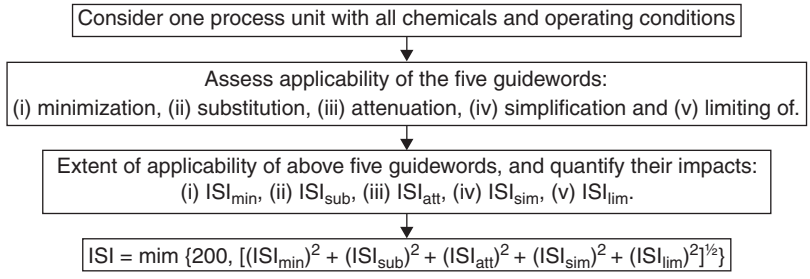

Figure 16.5 *Flowchart for ISI calculation for each process unit (Khan and Amyotte, 2004); ISI—inherent safety index; ISI_{min}—ISI for minimization; ISI_{sub}—ISI for substitution; ISI_{att}—ISI for attenuation; ISI_{sim}—ISI for simplification; v) ISI_{lim}—ISI for limiting of.*

16.3 Cumene Process, its Simulation and Costing

In the petrochemical industry, benzene and propylene are converted into more valuable phenol and acetone. Cumene, an important intermediate in this conversion, is produced by the reaction of benzene and propylene in a high-temperature and high-pressure gas phase reactor. Cumene also reacts with propylene to form p-diisopropyl benzene (PDIB) as a side product. These two reactions are as follows.

$$C_6H_6 + C_3H_6 \rightarrow C_9H_{12} \tag{16.2}$$

$$C_9H_{12} + C_3H_6 \rightarrow C_{12}H_{18} \tag{16.3}$$

Both these reactions are exothermic and irreversible in nature. Their reaction kinetics (Table 16.1) show that the activation energy of side reaction is larger than that of main reaction. A lower reactor temperature therefore favors cumene production, although the rate of reaction would be lower. Cumene selectivity will also be improved by low concentrations of cumene and propylene in the reactor to reduce the side reaction. This can be accomplished by using excess benzene, but it will require benzene recycling and hence additional cost of separation.

Turton *et al.* (2003) presented a process flow sheet for producing cumene using benzene and propylene, which has been optimized by Luyben (2010) for economic objectives. Luyben (2010) pointed out that the process economics dictate a high reactant conversion

Table 16.1 *Reaction kinetics of main and side reactions for cumene and PDIB production respectively (Turton* et al.*, 2003).*[a]

Kinetic parameter	Main reaction	Side reaction
Pre-exponential factor, A (kmol/m^3.s)	2.8×10^7	2.32×10^9
Activation energy, E (kJ/mol)	104 174	146 742
Concentration term (kmol/m^3)	$P_C B_C$	$P_C C_C$

[a]Component concentration is indicated by: P_C—propylene, B_C—benzene and C_C—cumene.

so as to minimize wastage of expensive raw materials. Higher conversion also leads to lower separation requirements in the downstream section, enabling the design of smaller distillation columns, reboilers and condensers, as well as smaller recycle flow rates. In the cumene process, propane is present as an impurity in the fresh propylene feed, and does not react in the process. As propane and propylene separation is difficult and uneconomical, both propane and unreacted propylene are flashed off and burned. As such, economics favor reactor design for high propylene conversion by either increasing reactor size (which increases capital cost) or using higher reaction temperature (which increases the amount of side product and hence material loss). Another point to note is that the side product, PDIB is also burned off and so has fuel value only; hence, its production should be kept as low as possible to minimize both material wastage and cost of separation. The tradeoffs mentioned above must be considered in the design of the cumene process.

An examination of cumene process flow sheet reveals that energy requirement for preheating of reactor feed stream is significantly large. In conjunction, reactor outlet stream is at high temperature (427 °C in Turton *et al.*, 2003), and it has to be cooled. In the process optimized by Luyben (2010), some energy is recovered from the reactor itself as high pressure steam (HPS), which reduces reactor outlet temperature to 358.5 °C. In this work, besides HPS production from the reactor, energy is recovered from the high temperature and pressure effluent of the reactor by expansion (to recover mechanical energy) followed by heat exchange with the reactor feed. This heat integration eliminates the fired heater and vaporizer used to preheat the feed in the cumene processes studied earlier (Turton *et al.*, 2003, and Luyben, 2010), and thus reduces capital and utilities costs. A fired heater of smaller capacity may be required for startup and control purposes. Increased heat integration makes process control more challenging. These aspects are not considered in the present chapter.

Turton *et al.* (2003) and Luyben (2010) have studied the cumene process with a capacity of 88.48 kilotons per annum (kTA). A typical cumene plant now produces up to 300 kTA of cumene. Hence, this study considers a scaled-up cumene process that can produce 300 kTA of cumene, which is equivalent to 37,500 kg/h of cumene production. This requires increasing different flow rates and sizes of equipments. Luyben (2010) has used NRTL thermodynamic model (i.e., fluid package) for simulating cumene process in Aspen Plus. The present study employs Aspen Hysys simulator. According to its guidelines, the Peng–Robinson fluid package is more suitable for this process as it involves hydrocarbons at high pressure. Hence, this study uses the Peng–Robinson fluid package for simulating cumene process in Aspen Hysys.

In the improved and scaled-up process for cumene (Figure 16.6), liquid feeds enter the process. Propylene (C3) feed has 95% propylene with the rest being propane, whilst benzene feed is assumed to be 100% pure. Fresh C3 and benzene flow rates are 350 and 330 kmol/h, respectively. The fresh benzene stream is combined with the recycled benzene stream. The mixed benzene and C3 feed, at 25 bar, enters the feed-effluent heat exchanger (FEHE), and leaves as a gas stream at 304.9 °C. This gas stream flows to the cumene reactor, which is a cooled tubular reactor to maintain an optimal reaction temperature and to recover some energy as HPS. The reactor effluent at 368.5 °C and 24.9 bar is expanded in a gas expander to 11.97 bar and 349.0 °C. It is then cooled to 87.4 °C by heat exchange with the feed stream in the FEHE. The cooled two-phase stream at the exit of FEHE is sent to a flash tank; the off-gas from this flash tank has high proportion of propylene and benzene

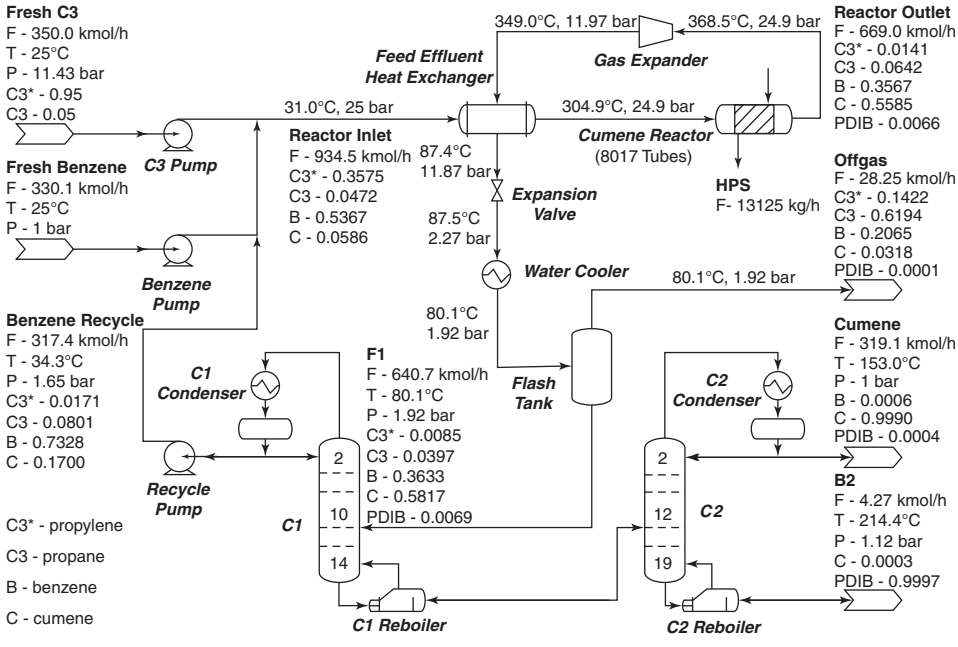

Figure 16.6 *Improved process with energy integration for 300,000 tons/year of cumene; stream data (i.e., flow rate, temperature, pressure and component mole fractions) correspond to the optimal solution "+" in Table 16.4.*

(∼14 and 21% respectively). The liquid phase from the flash tank is fed to the distillation column C1, to separate benzene from cumene and PDIB. The distillate having 73.3 mol% benzene is recycled and mixed with fresh benzene. The bottom stream from column C1 is fed to another distillation column C2, to produce 99.9 mol% cumene as the distillate. The bottom product from C2 consists of mostly PDIB, which represents a loss of reactants.

For sizing and costing, all pumps are assumed to be of the centrifugal type, all heat exchangers including condensers to be floating-head shell and tube type, and reboilers of C1 and C2 columns to be kettle type. The cumene reactor has been modeled as a kettle reboiler (to facilitate HPS production) having tubes of 0.0763 m diameter and 7.315 m long. The reactor tubes contain solid catalyst with a void fraction of 0.5 and solid density of 2000 kg/m^3 (Luyben, 2010); this catalyst has to be replaced every five years (Turton *et al.*, 2003). Finally, flash tank and distillation columns are considered as vertical pressure vessels. The construction material is assumed to be cast iron for pumps, carbon steel for heat exchangers, reboilers, flash tank, distillation columns and trays, and stainless steel 304 for both shell and tubes of the cumene reactor.

Total capital cost (TCC) is the one-time expense for the design, construction and startup of a new plant. The equipment-sizing equations and cost correlations from Seider *et al.* (2010) are used for estimating the TCC of cumene process; these cost correlations are for the Chemical Engineering Plant Cost Index (CEPCI) of 500. This study uses CEPCI of 600 as representative for the present time. The purchased cost (C_P) of a piece of equipment

is calculated using equations in Box 16.1. The total bare module cost (C_{TBM}) is then calculated using the following equation:

$$C_{TBM} = \sum_{\text{all equipments}} (C_p F_{BM}) + C_{catalyst} \tag{16.4}$$

where F_{BM} is the bare-module factor, which can be obtained from Seider *et al.* (2010). The cost of catalyst initially, and replacement every five years, is considered for the entire plant life of 20 years.

Box 16.1 Correlations for purchased cost of equipment (Seider et al., 2010; CEPCI = 500 unless otherwise stated).

Benzene feed pump, ethylene feed pump and recycle pump

$C_P = (F_{T,\,pump} F_M C_{B,\,pump} + F_{T,\,motor} C_{B,\,motor})$

$C_{B,\,pump} = \exp\{9.7171 - 0.6019\,[\ln(S)] + 0.0519\,[\ln(S)]^2\}$, where $S = Q(H)^{0.5}$

$C_{B,\,motor} = \exp\{5.8259 + 0.13141[\ln(P_C)] + 0.053255[\ln(P_C)]^2 + 0.028628[\ln(P_C)]^3 - 0.0035549[\ln(P_C)]^4\}$, where $P_C = QH\rho / (33{,}000\,\eta_P\eta_M)$

C_B—bare module cost, S—size factor, Q—flow rate (gallons/min), H—pump head (ft), P_C—power consumption (hp), ρ—density (lb/gallon), F_T—pump type factor, F_M—material factor, η_P—pump fractional efficiency, η_M—motor fractional efficiency.

FEHE, water cooler and condensers of columns C1 and C2 (floating head shell and tube heat exchangers)

$C_P = F_P F_M F_L C_B$, $C_B = \exp\{11.9052 - 0.8709[\ln(A)] + 0.09005[\ln(A)]^2\}$

$F_M = 1$, A—tube outside surface area (ft^2), F_P—pressure factor, F_L—tube length correction factor

Cumene reactor and reboilers of columns C1 and C2 (kettle reboiler); base CEPCI = 394

$C_P = F_P F_M F_L C_B$, $C_B = \exp\{11.967 - 0.8709[\ln(A)] + 0.09005[\ln(A)]^2\}$

$F_M = a + (A/100)^b$, where a and b are constants based on construction material, A—tube outside surface area (ft^2), F_P—pressure factor, F_L—tube length correction factor

Expander (gas expander)

$C_P = \{-98.328[\ln(P_C)] + 1318.5\}P_C$, P_C—power consumption (hp)

Flash tank (vertical pressure vessel)

$C_P = (F_M C_V + C_{PL})$

$C_V = \exp\{7.0132 + 0.18255[\ln(W)] + 0.02297[\ln(W)^2]\}$, for $4{,}200 < W < 1{,}000{,}000$ lbs

$C_{PL} = 361.8(D_i)^{0.7396}(L)^{0.70684}$, for $3 < D_i < 21$ ft and $12 < L < 40$ ft

$F_M = 1$, $W = \pi(D_i + t_S)(L + 0.8D_i)t_S\rho$, L—tangent-to-tangent length of shell (ft), t_S—shell thickness (in)

Columns C1 and C2 (tower with trays)

$C_P = (F_M C_V + C_{PL} + C_T)$

$C_V = \exp\{7.2756 + 0.18255[\ln(W)] + 0.02297[\ln(W)]^2\}$, for $9{,}000 < W < 2{,}500{,}000$ lbs

$C_{PL} = 300.9(D_i)^{0.63316}\,(L)^{0.80161}$, for $3 < D_i < 24$ ft and $27 < L < 170$ ft

$C_T = N_T F_{NT} F_{TT} F_{TM} C_{BT}$, $C_{BT} = 468\exp(0.1739\,D_i)$

N_T—number of trays, F_{NT}—factor depending on number of trays, F_{TT}—factor depending on type of trays, F_{TM}—correction factor for tray construction material

Total direct permanent investment (C_{DPI}) is evaluated using the following relation:

$$C_{DPI} = C_{TBM} + C_{site} + C_{serv} + C_{alloc} \tag{16.5}$$

Here, C_{DPI} includes site preparation cost ($C_{site} = 0.2C_{TBM}$), cost for service facilities (C_{serv}—assumed negligible), and allocated capital cost for facilities related to utilities (C_{alloc}) that can be calculated based on the information provided in Seider *et al.* (2010). Total depreciable capital (C_{TDC}) is found by adding C_{DPI} to contingencies and contractor fee ($C_{cont} = 0.18C_{DPI}$).

$$C_{TDC} = C_{DPI} + C_{cont} \tag{16.6}$$

Total permanent investment (C_{TPI}) is the sum of $C_{TDC,}$ cost of land ($= 0.02C_{TDC}$), royalties ($= 0.02C_{TDC}$), and startup ($= 0.1C_{TDC}$).

$$C_{TPI} = C_{TDC} + C_{land} + C_{royal} + C_{startup} \tag{16.7}$$

Finally, C_{TPI} and working capital (C_{WC}) are added to obtain TCC:

$$TCC = C_{TPI} + C_{WC} \tag{16.8}$$

16.4 I2SI Calculation for Cumene Process

In the SWeHI approach, various process units are classified into five categories, namely storage, physical operation, chemical reaction, transportation, and other hazardous units. This work considers only physical operations and chemical reaction units in the I2SI calculation, as other hazardous units are not present in the cumene process and storage/transportation facilities are unlikely to be affected by the process design. Although a robust and comprehensive index, the I2SI has certain shortcomings. In the calculation of ISI, the value of each guideword is estimated based on its applicability, which is subjective and difficult to quantify (Khan and Amyotte, 2004). Similarly, PHCI calculation requires ranking of certain parameters, which relies on personal views of process safety experts. Although ISI and PHCI depend on the experience of experts, assigned values for them will be fixed for a process, irrespective of the design and operating conditions. Hence, these two are omitted in the calculation of I2SI for the preliminary design and optimization of cumene process. Thus, I2SI calculation is reduced to DI calculation (Figure 16.1), and minimization of DI is equivalent to maximization of I2SI (i.e., better inherent safety of the process).

16.4.1 FEDR Calculation for Units Involving Physical Operations

For FEDR calculation, three energy factors: F1, F2 and F3 are defined for each chemical in a physical operation unit, and later used in the calculation of hazard potential (see Equation 16.12). The F1 factor accounts for chemical energy, whereas the F2 and F3 factors account for physical energies:

$$F1 = 0.1M_f \frac{H_c}{K} \tag{16.9}$$

$$F2 = 1.304 \times 10^{-3} P_P V \tag{16.10}$$

$$F3 = \frac{1.0 \times 10^{-3}}{T + 273}(P_P - V_P)^2 V \tag{16.11}$$

In Equation 16.9, M_f is the mass flow rate of the chemical (kg/s), H_c is the heat of combustion of the chemical (kJ/mol), and K (= 3.148) is a constant. In Equations 16.10 and 16.11, P_P (kPa) and V_P (kPa) are the process pressure and vapor pressure of the chemical at process temperature T (°C) respectively. V is the volumetric flow rate of chemical (m^3/h).

Penalties, pn1 to pn8, are assigned to evaluate the impacts of different factors on FEDR (Khan *et al.*, 2001): pn1 measures the effect of operating temperature, flash point, fire point and autoignition point of the chemical; pn2 determines the effect of process pressure by comparing it against vapor pressure of the chemical at process temperature and atmospheric pressure. NFPA ranking for flammability (NF) and reactivity (NR) are used to calculate pn3; pn4 evaluates the effect of chemical characteristics, in particular flammability and reactivity; pn5 quantifies impacts of a hazardous unit on its neighboring units; in this work, the maximum value of pn5 is used because the relative location of neighboring units is unlikely to be known at the preliminary design stage; pn6 accounts for the density of units based on the percentage of space occupied by an individual unit within an area of 30 m radius; in this work, space density of 25% is assumed, as in the illustrative example in Khan *et al.* (2001). To approximate the effects of external factors such as earthquakes and hurricanes, pn7 uses the predicted occurrence frequencies of these events. Finally, pn8 estimates the vulnerability of the surroundings by assigning a maximum value of 2 for an area that is prone to accidents or 1.1 otherwise.

Mathematical formulation with detailed discussion and calculation for the above penalties can be found in Khan *et al.* (2001); an outline of this is given in Appendix A.1. Hazard potential of a process unit involving physical operations can be calculated using Equation 16.12. After that, FEDR is calculated according to Equation 16.13.

$$\text{Hazard Potential} = (\text{F1} \times \text{pn1} + \text{F} \times \text{pn2}) \times \text{pn3} \times \text{pn4} \times \text{pn5} \times \text{pn6} \times \text{pn7} \times \text{pn8} \quad (16.12)$$

$$\text{FEDR} = 4.76(\text{Hazard Potential})^{1/3} \quad (16.13)$$

In Equation 16.12, F is determined by comparing the vapor, ambient and process pressures: (i) for vapor pressure > ambient pressure, if process pressure > vapor pressure then F = F2 + F3 else F = F2; and (ii) for vapor pressure < ambient pressure, F = F3. Note that F2 and F3 are from Equations 16.10 and 16.11, respectively.

For a unit, FEDR for each chemical is calculated at inlet (and also outlet, if different) conditions; it is assumed that the maximum of these values is the FEDR for that unit (Adu *et al.*, 2008). This procedure is used for units involving physical operations, namely, benzene feed, propylene feed and recycle pumps, FEHE, gas expander, water cooler, flash tank and two distillation columns in the cumene process. The cumene reactor is the only unit involving a chemical reaction. FEDR for each chemical in both reactor inlet and outlet streams is evaluated following the procedure in the next subsection. Of these, the maximum value is the FEDR for the cumene reactor.

16.4.2 FEDR Calculation for Units Involving Chemical Reactions

For units involving chemical reactions, four energy factors and ten penalty factors are required for the calculation of the hazard potential. In addition to F1, F2 and F3 (in

Equations 16.9 to 16.11), one more energy factor (F4) is defined to represent the energy released due to chemical reaction, H_{rxn} (kJ/kg).

$$F4 = M_f \frac{H_{rxn}}{K} \tag{16.14}$$

As defined earlier, M_f is the mass flow rate of the chemical (kg/s), and $K = 3.148$.

In addition to eight penalties (pn1 to pn8) in previous subsection, two more penalties are defined. pn9 is related to the nature of reactions (e.g., alkylation for cumene process), and pn10 quantifies the impact of a side reaction by considering its probability and type (e.g., autocatalytic reaction for the cumene process). Finally, the hazard potential of each unit involving chemical reactions is calculated as follows:

$$\begin{aligned}\text{Hazard Potential} = (F1 \times pn1 + F \times pn2 + F4 \times pn9 \times pn10)\, pn3 \times pn4 \\ \times pn5 \times pn6 \times pn7 \times pn8\end{aligned} \tag{16.15}$$

The hazard potential of a process unit involving chemical reactions is converted to FEDR using Equation 16.13.

16.4.3 TDR Calculation

The computation of TDR involves the calculation of the G factor and seven penalties. The G factor accounts for the amount of chemical released and the release conditions, as follows.

$$G = S \times m \tag{16.16}$$

Here, S describes release conditions (see Table 16.2), and m is the chemical release rate (kg/s).

Seven penalties (pnr1 to pnr7) are used to quantify impacts of different operating conditions and other parameters. pnr1 measures the effect of operating temperature by considering flammability and/or toxicity of a chemical. For each chemical in a process unit, the value of pnr1 is assigned by comparing the process temperature with flash, fire and auto-ignition points of that chemical. pnr2 evaluates the effect of operating pressure by comparing it with the vapor pressure at the process temperature and ambient pressure. pnr3 considers dispersion of chemicals in the surroundings; denser gases require more time to disperse, which gives a higher toxic load near to site for a longer period of time. pnr3 quantification requires the vapor density of a chemical at release conditions and the ambient air density. pnr4 quantifies toxicity of each chemical using NFPA health factor (NH) as the assessment

Table 16.2 *Guideline to assign the value of S factor (Khan* et al.*, 2001).*

	S factor			
NFPA rank	Liquid	Liquefied gas	Gas	Solid
4	4	8	13.4	0.13
3	0.4	0.8	1.34	0.013
2	0.2	0.4	0.67	0.006
1	0.07	0.1	0.25	0.0025

criteria. The toxic penalties 5 to 7 account for the effect of site characteristics and surroundings. pnr5 is related to population density, and a maximum value of 1 is assigned to pnr5, if required information is not available. Pnr6 and pnr7 estimate effects of external factors and vulnerability of the area, respectively. Detailed calculations for the above penalties can be found in Khan *et al.* (2001), and an outline of them is given in Appendix A.2. Finally, TDR for the process is calculated using the following equation:

$$\text{TDR} = \text{a}(\text{G} \times \text{pnr1} \times \text{pnr2} \times \text{pnr3} \times \text{pnr4} \times \text{pnr5} \times \text{pnr6} \times \text{pnr7})^{\text{b}} \qquad (16.17)$$

Here, a (= 25.35) and b (= 0.425) are constants. Like FEDR, TDR is calculated for each and every chemical in a unit, and finally maximum of them is TDR for that unit.

16.4.4 Conversion of FEDR to FEDI, and TDR to TDI

After the calculation of FEDR and TDR, FEDI and TDI are estimated using figures in Khan and Amyotte (2004). The same value of TDR is used to calculate TDI for chronic toxicity (TDI_{CH}) and acute toxicity (TDI_{AC}). These two TDI values are combined to give the overall TDI, as follows:

$$\text{TDI} = \left[(\text{TDI}_{\text{CH}})^2 + (\text{TDI}_{\text{AC}})^2\right]^{1/2} \qquad (16.18)$$

The FEDI for individual process units are added to obtain total FEDI; the same procedure is used for the total TDI. Finally, the DI is calculated using total FEDI, total TDI and the following equation:

$$\text{DI} = \left[(\text{total FEDI})^2 + (\text{total TDI})^2\right]^{1/2} \qquad (16.19)$$

Note that FEDI and TDI values of a unit may come from either inlet or outlet stream, and from different chemicals.

16.5 Optimization using EMOO Program

The Microsoft Excel-based MOO (EMOO) program (Sharma *et al.*, 2011) is used to generate the tradeoff solutions for cumene process. It uses the elitist non-dominated sorting genetic algorithm (NSGA-II) along with binary coding of decision variables, and handles inequality constraints by the constrained dominance approach, also known as the feasibility approach (Deb *et al.*, 2002). Equality constraints, if present, need to be transformed into inequality constraints (see Chapter 5 of this book for more details).

Figure 16.7 shows a flowchart of NSGA-II and its implementation in the EMOO program. In this, a population of NP individuals is randomly initialized inside the bounds on decision variables. In each generation, two individuals from the current population are selected using binary tournament, for reproduction operation. New individuals are generated by crossover and mutation of these selected individuals. The newly generated individuals are checked for violation of decision variable bounds; if there is a violation, then that decision variable of the new individual is randomly reinitialized inside the bounds on that decision variable. Thus, NP new individuals are generated and then combined with the parent population. Non-dominated sorting of the combined population is performed to rank all individuals according to constrained dominance approach (Deb *et al.*, 2002), which

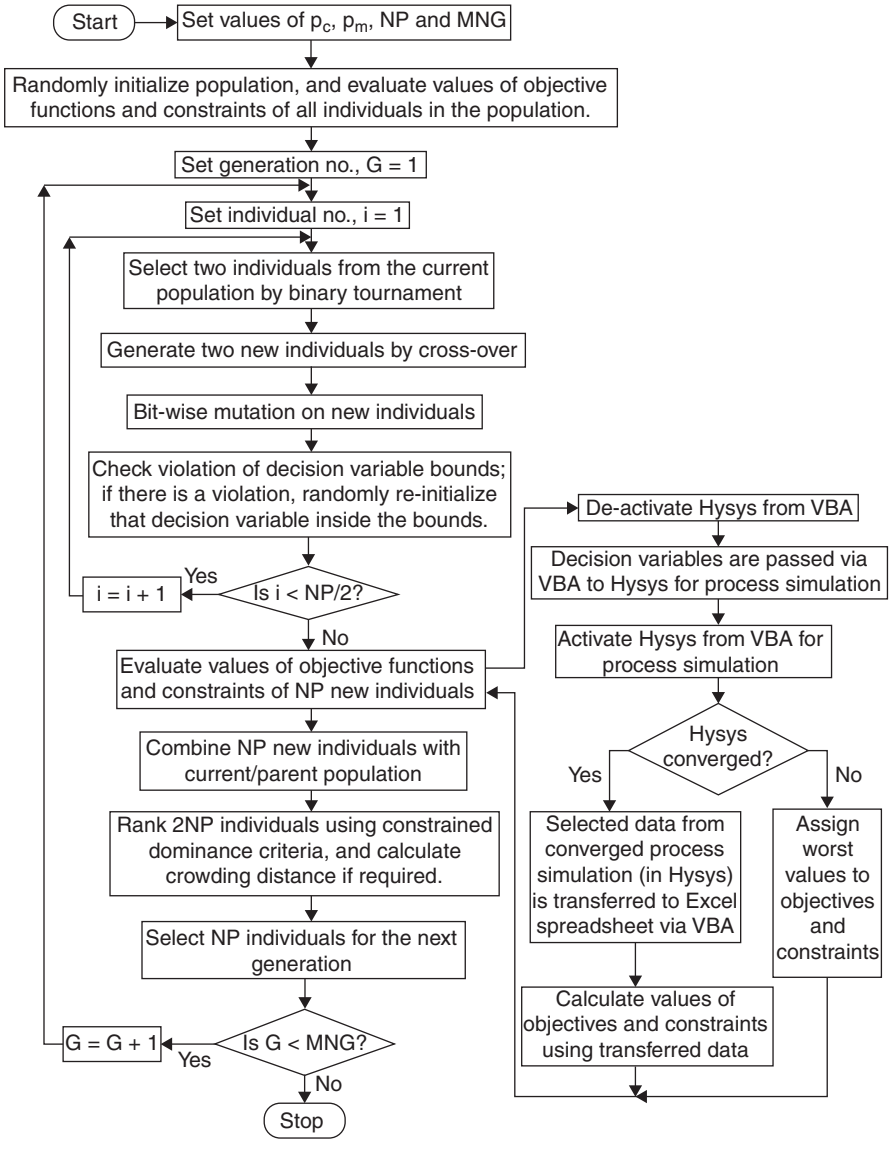

Figure 16.7 *Flowchart of MOO algorithm (NSGA-II) and its implementation for this work using Aspen Hysys for process simulation.*

gives higher priority for feasibility over objective function values. Individuals from the best fronts (first, second, third, etc.) are selected for the subsequent generation; if all individuals of the same rank cannot be selected, then crowding distances are calculated for each of them, and the least crowded individuals are selected to complete the NP individuals for the subsequent generation. Iterations are repeated for the maximum number of generations (MNG).

NSGA-II algorithm has been coded in Excel Macro using Visual Basic for Applications (VBA) language. The user can provide objective functions, constraints, decision variables and their bounds, and also specify NSGA-II parameters such as crossover probability ($p_c = 0.9$), mutation probability ($p_m = 0.01$), population size (NP = 100) and maximum number of generations (MNG = 100), through a user-interface worksheet. EMOO program is interfaced with Aspen Hysys using VBA. A vector of decision variables is passed to Aspen Hysys, and process simulation is activated (see Figure 16.7). After the convergence of simulation, the required simulation results are transferred to Excel; these are used to calculate the values of objectives and constraints in the Excel worksheet.

16.6 Optimization for Two Objectives

As discussed in section 16.4, I2SI for the preliminary design of cumene process can be reduced to the DI calculation. The maximization of I2SI is equivalent to the minimization of DI (see Figure 16.1), and hence DI is directly used as the safety objective function in the present MOO study. In the calculation of DI, fire and explosion, acute toxicity, and chronic toxicity hazards are considered; that is, environmental hazard is excluded because a separate environmental criterion is used to assess the environmental impact. Further, material mass flow rate (kg/s) is used for calculating DR in Figure 16.3 because SWeHI methodology can use total inventory or mass flow rate (Khan *et al.*, 2001), and Adu *et al.* (2008) have used maximum of mass flow rate at the reactor inlet and outlet for health and safety assessment.

Preliminary MOO studies on the cumene process showed that TCC is a suitable economic criterion due to its sensitivity to decision variables. Hence, TCC is chosen as the economic objective in this study. Emission of hydrocarbons is used to represent the environmental impact of the cumene process. This process (Figure 16.6) has material losses in the off-gas from flash tank and in the bottom product from C2 column. Minimization of benzene and propylene flow rates in the off-gas implies a better utilization of raw materials, while minimization of cumene flow rate in the off-gas reduces the loss of valuable product. Further, minimization of mass flow rate of C2 bottoms identifies operating conditions that favor the main reaction. Therefore, the objective is to minimize the emissions of benzene, propylene and cumene in the off-gas, together with PDIB in the C2 bottom product.

In this work, the cumene production rate (CPR) fluctuates slightly above the minimum value of 37,500 kg/h. Hence, normalized DI, TCC and material loss using CPR are considered as the objectives, which enable comparison of different non-dominated solutions on a similar basis. Moreover, preliminary optimization results obtained with and without normalization showed that the latter has relatively more variability with decision variables. In order to analyze the effect of including mass information, Adu *et al.* (2008) also have compared different process routes using the normalized safety index.

Table 16.3 presents objectives, decision variables and constraints in different MOO problems studied. Note that flow rate of propylene feed (containing 95 mol% propylene and 5 mol% propane) is constant at 350 kmol/h. Decision variables and their ranges in Table 16.3 have been determined through preliminary trials. The lower bound of benzene flow rate ensures the required production capacity, while its upper bound avoids excessive loss of benzene and high recycle-flow rate. The range of reactor inlet temperature allows a reasonable reaction rate, while the reactor outlet temperature range decides the amount of

Table 16.3 *Formulation of different MOO problems.*

Objectives	Decision variables	Constraints
(A) min DI/CPR, min material loss/CPR	$330 \leq$ benzene flow rate ≤ 360 kmol/h $290 \leq$ reactor inlet temperature ≤ 320 °C $348.5 \leq$ reactor outlet temperature ≤ 368.5 °C	$LMTD_{FEHE} > 10$ °C $LMTD_{water\ cooler} > 10$ °C $LMTD_{C1\ cond/reb} > 10$ °C
(B) min TCC/CPR, min material loss/CPR	$800 \leq$ expander outlet pressure $\leq 1{,}200$ kPa $209.5 \leq$ valve outlet pressure ≤ 229.5 bar $80 \leq$ cooler outlet temperature ≤ 90 °C	$LMTD_{C2\ cond/reb} > 10$ °C $\Delta T_{cooler} > 2$ °C recycle flow to feed ratio < 4
(C) min DI/CPR, min TCC/CPR	$8{,}000 \leq$ reactor tube count $\leq 12{,}000$ $0.4 \leq$ C1 reflux ratio ≤ 0.48	F1 propylene content < 0.05
(D) min material loss/CPR, min TCC/CPR, min DI/CPR	$0.0004 \leq$ benzene mole fraction in C1 bottom ≤ 0.0006 $0.67 \leq$ C2 reflux ratio ≤ 0.72	CPR $> 37{,}500$ kg/h

Note: material loss is combined flow rates of benzene, propylene and cumene in off-gas, and of PDIB in C2 bottom product.

steam generated and the extent of side reaction (which are favored by high temperature). Further, the reactor tube count affects reaction conversion.

The expander outlet pressure decides the amount of mechanical energy recovered via expansion of the reactor outlet stream. A feasible operation of flash tank is ensured by suitable ranges of valve outlet pressure and cooler outlet temperature. Ranges of C1 and C2 reflux ratios and benzene mole fraction in C1 bottom are decided based on the required purity of product. Constraints are included to ensure the feasibility of production process. A minimum log-mean temperature difference (LMTD) in heat exchangers provides adequate driving force and avoids very large heat exchangers. A minimum temperature change in process stream across the cooler prevents convergence problem in Aspen Hysys, whereas a maximum recycle flow to feed ratio avoids process design that may require significantly high cost. The constraint for CPR ensures the required production capacity.

16.6.1 Tradeoff between DI and Material Loss

Figure 16.8(a) shows the Pareto-optimal front obtained for normalized DI and normalized material loss. Both objectives cover reasonable ranges; the normalized DI shows about 2% variation while the normalized material loss has a variation of about 13%. In this and other cases studied, CPR varies by 1–2%. Here, the Pareto-optimal front initially shows a steep change in the normalized material loss with a small change in normalized DI, followed by a larger change in normalized DI with a small change in normalized material loss (Figure 16.8a). So, the Pareto-optimal front has a corner solution that may be preferred in the decision making.

In this case, the two objectives are mainly affected by benzene flow rate (Figure 16.8b). It can be seen that an increase in benzene flow rate results in an increase in the normalized DI and a relatively large decrease in the normalized material loss. A higher benzene flow rate

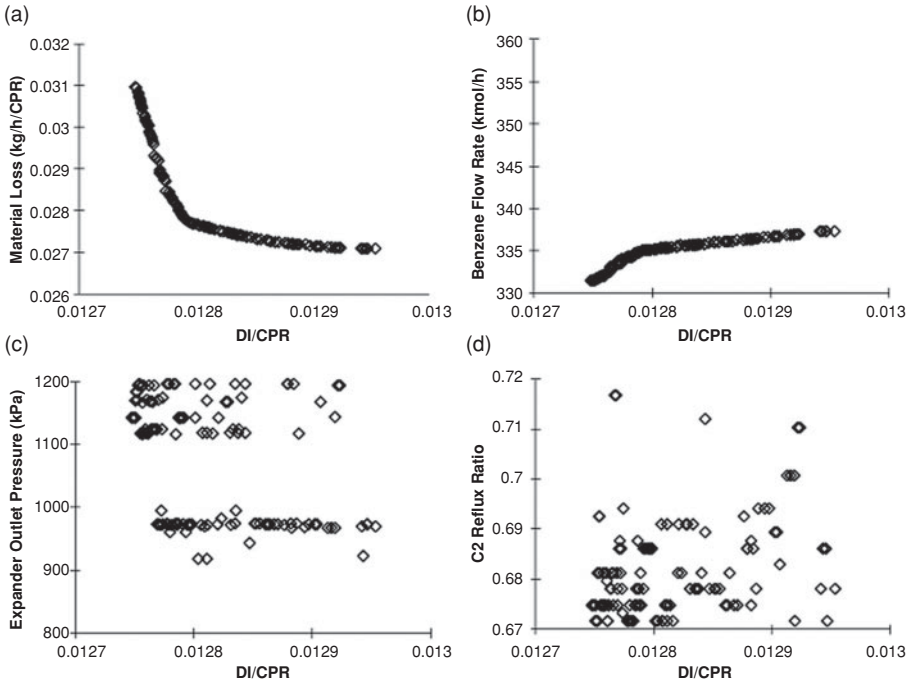

Figure 16.8 *Selected optimization results for simultaneous minimization of normalized DI and normalized material loss; CPR—cumene production rate (kg/h).*

increases overall mass flow rate throughout the process; naturally, this increases the hazard potential, and hence normalized DI. Further, an excess of benzene in the feed lowers the concentrations of cumene and propylene in the reactor, which improves the selectivity of the main reaction over the side reaction. The DI also increases due to improved selectivity, as cumene has the largest DI among all chemicals for all process units except the three pumps, in the cumene process. Further, higher consumption of propylene lowers the amount of off-gas from the process. The normalized material loss is further reduced due to lower production of the side product (PDIB). It can be seen that the sharp increase in benzene flow rate corresponds to the steep initial decrease in normalized material loss (Figures 16.8a–b). Coupled with the small variation in CPR, a higher benzene flow rate gives higher DI/CPR and a lower material loss/CPR.

The expander outlet pressure and C2 reflux ratio are scattered within the bounds (see Figures 16.8c–d). The other decision variables remain nearly constant, and so they are not shown for brevity. Reactor outlet temperature (∼368.5 °C), valve outlet pressure (∼229.5 kPa), reactor tube count (∼12,000), C1 reflux ratio (∼0.48) and benzene mole fraction in C1 bottom (∼0.0006) are near to their upper bounds. Reactor inlet temperature is in its middle range (∼305 °C) while cooler outlet temperature is near its lower bound (∼80 °C). These results are useful for further improving Pareto-optimal solutions by relaxing one or more bounds on decision variables, if there is a possibility.

16.6.2 Tradeoff between TCC and Material Loss

The Pareto-optimal front obtained for normalized TCC and normalized material loss is shown in Figure 16.9(a). As expected, these two objectives are conflicting in nature—an increase in one objective is accompanied by a decrease in the other objective. TCC/CPR and material loss/CPR have variation of about 33% and 34% respectively; such significant variations in objectives indicate pronounced effects of decision variables. The Pareto-optimal front has a steep initial change in normalized TCC, followed by a steep change in normalized material loss (Figure 16.9a).

The main decision variables affecting both normalized TCC and normalized material loss are benzene flow rate, reactor inlet temperature, and reactor tube count (see Figure 16.9). The initial variation in both normalized objectives is independent of benzene flow rate and reactor inlet temperature (see Figures 16.9a–c). Later, both benzene flow rate and reactor inlet temperature affect material loss/CPR to a larger extent (i.e., beyond material loss/CPR of 0.033). Lower values of both decision variables give lower conversion in the reactor. As the amount of unreacted propylene increases, a larger amount of off-gas is flashed off. This results in higher material loss/CPR. The lower throughput to downstream process also enables the use of smaller equipment, which lowers TCC/CPR.

The steep initial change in the normalized TCC (i.e., before material loss/CPR of 0.033) is mainly due to the reactor tube count as shown in Figure 16.9(e). The TCC is significantly affected by the cost of the cumene reactor. The normalized TCC therefore changes with the number of reactor tubes. Moreover, as the tube count decreases, conversion in the reactor decreases. A corresponding higher amount of unreacted propylene leads to a greater amount of off-gas vented and consequently normalized material loss.

The C2 reflux ratio is scattered within its bounds (see Figure 16.9h). Valve outlet pressure (Figure 16.9d), C1 reflux ratio (Figure 16.9f) and the benzene mole fraction in C1 bottom (Figure 16.9g) are mostly close to their respective upper bound, with some solutions scattered near the upper bounds. Reactor outlet temperature ($\sim$368.5 °C), expander outlet pressure ($\sim$1200 kPa) are near to their respective upper bound while cooler outlet temperature ($\sim$80 °C) is largely invariant near its lower bound; these are not shown in Figure 16.9 for brevity.

16.6.3 Tradeoff between DI and TCC

In the Pareto-optimal front obtained for the normalized DI and the normalized TCC (Figure 16.10a), DI/CPR shows a variation of 1%, while TCC/CPR has a variation of about 31%. The reactor tube count is mainly affecting both the objectives; a larger number of tubes in the reactor leads to a higher TCC/CPR and lower DI/CPR (Figures 16.10a and 16.10c). Variation in the normalized TCC with the reactor tube count is similar to the optimization results obtained for economic and environmental objectives in the previous subsection. Further, a large cumene reactor gives higher conversion, which lowers the separation requirement in the downstream section. The recycle flow rate is small for high conversion in cumene reactor, and recycle flow has a positive impact on the normalized DI. Overall, the DI/CPR value is marginally lower for larger number of reactor tubes. Valve outlet pressure is scattered within its lower and upper bounds (Figure 16.10b), the C2 reflux ratio is scattered near to its lower bound (Figure 16.10d). Cooler outlet temperature is nearly constant at its lower bound (i.e., 80 °C). Reactor outlet temperature ($\sim$368.5 °C), expander

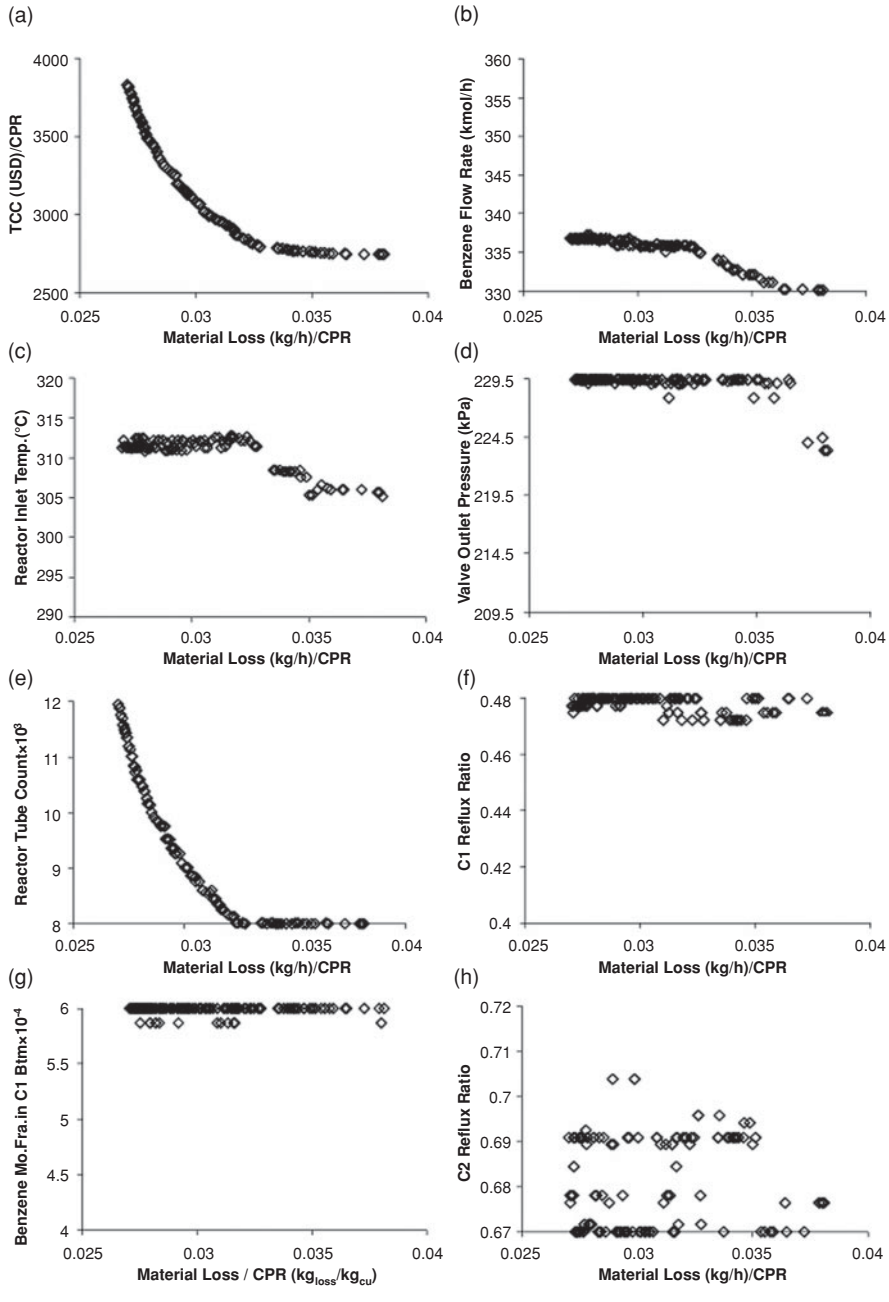

Figure 16.9 *Selected optimization results for simultaneous minimization of normalized TCC and normalized material loss; CPR—cumene production rate (kg/h).*

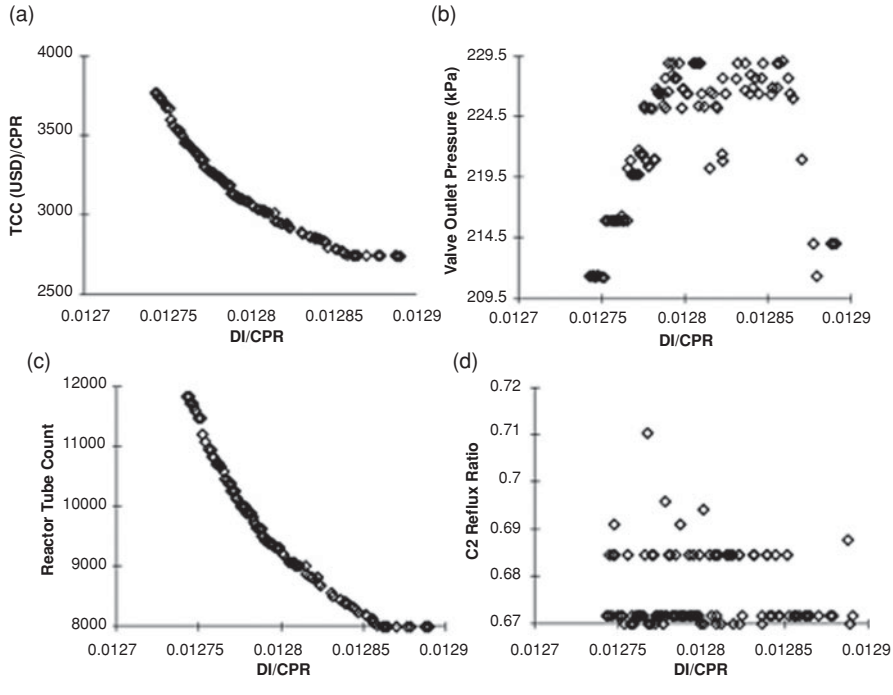

Figure 16.10 *Selected optimization results for simultaneous minimization of normalized DI and normalized TCC; CPR—cumene production rate (kg/h).*

outlet pressure (∼1200 kPa), C1 reflux ratio (∼0.48) and benzene mole fraction in C1 bottom (∼0.0006) are near to their respective upper bound. The reactor inlet temperature (∼305 °C) is in between its bounds while fresh benzene flow rate (∼330 kmol/h) is closer to its lower bound. For brevity, these results are not shown in Figure 16.10.

16.7 Optimization for EES Objectives

Figures 16.11(a) and (b) show the Pareto-optimal front obtained for normalized TCC, normalized material loss and normalized DI, which vary by approximately 31%, 33% and 2%, respectively. Figures 16.11(c) to 16.11(h) present the variations in some of the decision variables. In particular, the Pareto trend in Figure 11(a) is similar to variation in the reactor tube count with normalized material loss (Figure 16.11f). Appendix A.3 provides two different 3-D plots for the non-dominated solutions obtained in this tri-objective optimization. These plots show variations in each objective, and the source file (in MATLAB) for these plots is available on the book's web site, for better visualization of the 3-D plot.

In order to analyze MOO results for three objectives, four non-dominated solutions from the Pareto-optimal front are chosen (see Figure 16.11), and the optimal values of objectives for these are reported in Table 16.4. It can be seen that, for solution "+," the highest

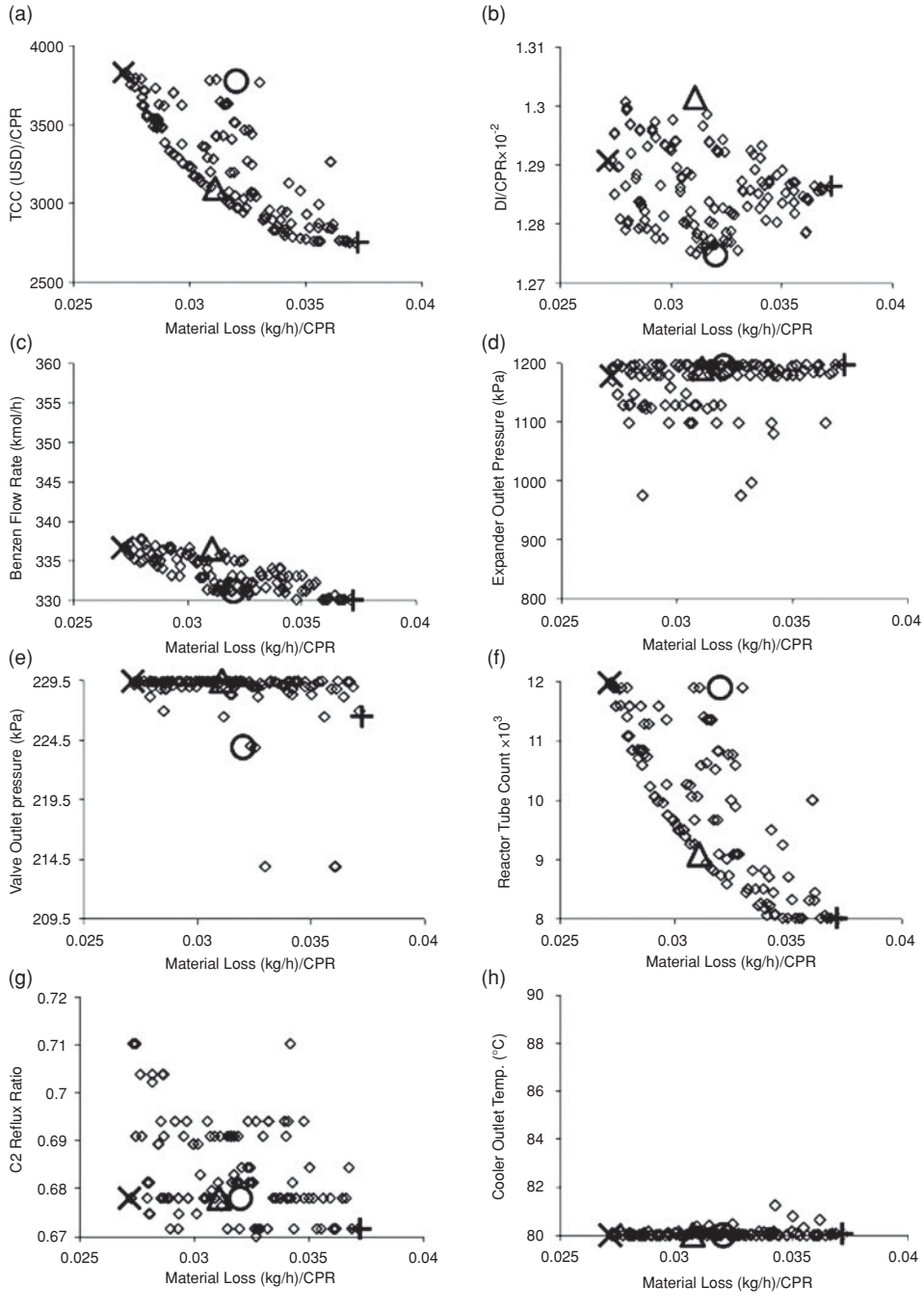

Figure 16.11 *Selected optimization results for simultaneous minimization of TCC, material loss, and DI (all normalized); CPR—cumene production rate (kg/h).*

Table 16.4 *Optimal values of objective functions for four selected non-dominated solutions in Figures 11(a) and 11(b); CPR—cumene production rate (kg/h).*

Pareto-optimal solution	TCC (USD)/CPR	Material loss (kg/h)/CPR	DI/CPR
"+"	2749	0.03723	0.01286
"×"	3829	0.02714	0.01291
"Δ"	3095	0.03107	0.01301
"O"	3776	0.03200	0.01275

normalized material loss corresponds to the lowest normalized TCC and medium normalized DI. Conversely, for solution "×", the lowest normalized material loss corresponds to the highest normalized TCC and medium normalized DI. The highest normalized DI (solution "Δ") is achieved for medium values of both economic and environmental objectives. Solution "O" has the lowest normalized DI at the expense of medium values of both normalized TCC and material loss.

Despite small variation in normalized DI, its evaluation is essential. In view of more stringent safety guidelines and industry standards, an increase in DI can lower inherent safety and warrant significant changes to the process design. Furthermore, minimization of safety hazards within a chemical plant is linked to reduction of future maintenance and/or damage costs, which are not considered in the initial investment (i.e., TCC). Optimization using DI as a safety objective also allows engineers to identify the key areas that affect inherent safety. For example, in the cumene process, benzene flow rate and reactor inlet temperature can be lowered to achieve a lower normalized DI, thus improving inherent process safety.

16.8 Conclusions

This chapter explored tradeoffs among three different types of objectives (economic, environmental, and safety) for a cumene production process. The EMOO program, based on the elitist NSGA-II, is used successfully to generate Pareto-optimal fronts. MOO provides optimal values of objectives and decision variables, which are useful for selecting an optimal solution and/or for further optimization. For example, a corner solution present on the Pareto-optimal front can be chosen for practical implementation.

As expected, all the three objectives (i.e., TCC, material loss and DI) for the cumene process are conflicting in nature. Improvement in inherent process safety and reduction in material loss are associated with a larger capital investment. Identification of critical decision variables and their effects on objective functions through MOO give better insights about the process, which helps engineers to achieve substantial improvements. For the cumene process, a higher benzene feed flow rate increases both TCC and DI. Further, a higher benzene feed-flow rate and reactor inlet temperature decrease material loss from the process. Reactor tube count is another important decision variable; TCC increases with higher reactor tube count, while the DI and material loss follow opposite trends.

In general, the safety objective used in this work (i.e., DI or I2SI) can be applied to other chemical processes. The I2SI can be further improved by capturing all the important aspects

of process safety using knowledge of the process conditions and the chemicals involved. Possible improvements include the development of alternative methods to evaluate the subjective components that have been omitted from the I2SI calculation in this study.

Acknowledgments

The authors acknowledge Chia Bing Cheng, Frankie for his initial work in this area and for his help during the work described in this chapter.

Exercises

16.1. Alternative process flow sheets for cumene are available in Turton *et al.* (2003) and Luyben (2010). Explore the tradeoff among EES objectives for one or both of these, and compare the optimization results with those for the cumene process (Figure 16.6) presented in this chapter.

16.2. Choose a chemical process (for example, ammonia production, which involves high temperatures and pressures). Identify the process units involved in this process for their relative safety based on properties of chemicals, inventory and operating conditions. Optimize the chosen process for two or three EES objectives, and discuss the tradeoff among these objectives.

Appendices

A.1 Penalty Calculation for FEDR (Khan *et al.*, 2001)

- pn1 (effect of temperature):
  The pn1 parameter can be calculated based on Figure 16.A1. It is determined by comparing process temperature against the flash, fire and auto-ignition points. If flash or auto-ignition point of a chemical is unavailable, pn1 = 1. If fire point is unavailable, pn1 = 1.75 for flash point < process temperature < 0.75(auto-ignition point).

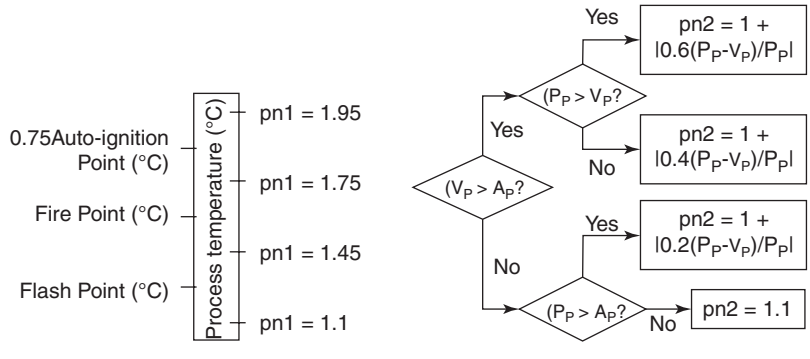

Figure 16.A1 *Calculation of pn1 (left plot) and pn2 (right plot) for FEDR.*

- pn2 (effect of pressure):
  The parameter, pn2 can be calculated based on Figure 16.A1. Here, A_P—ambient pressure (kPa), P_P—process pressure (kPa), V_P—vapor pressure (kPa).
- pn3 (quantity of chemicals):
  In the calculation of penalties, NFPA ranking (NF, NH and NR values) for each chemical can be obtained from its material safety data sheet (MSDS; http://cameochemicals.noaa.gov).

Maximum (NF, NR)	pn3 (empirical equations obtained based on graphs in Khan *et al.*, 2001)	Remarks
4	0.0102 × chemical inventory (tons) + 0.9936	• Empirical equations are valid for 10 ≤ chemical inventory ≤ 150 tons • If chemical inventory < 10 tons, then pn3 = 1.
3	0.0076 × chemical inventory (tons) + 0.9956	
2	0.0051 × chemical inventory (tons) + 0.9935	
1	0.0026 × chemical inventory (tons) + 0.992	
0	1	

- pn4 (chemical characteristics):
  pn4 = Maximum[1, 0.3 × (NR + NF)].
- pn5 (location of nearest hazardous unit):
  pn5 = 1.955 for d < 5, pn5 = $2.55/d^{0.165}$ for 5 ≤ d < 75 m, and pn5 = $2.0867/d^{0.11}$ for 75 ≤ d≤ 155 m, where d is the distance of nearest hazardous unit.
- pn6 (density of units):
  pn6 = 1 + fraction of space occupied by units in an area of 30 m radius (assuming current unit is at the centre of the circle)
- pn7 (external factors, like occurrence of disasters):
  pn7 = 2, 1.5 and 1.1 for disasters occurring once in a year, 5 years and 20 years, respectively.
- pn8 (vulnerability of surrounding):
  pn8 = 2 for an area that is prone to accidents, and 1.1 otherwise.
- pn9 (type of reaction):

Reaction type	pn9	Reaction type	pn9	Reaction type	pn9
Oxidation	1.60	Esterification	1.25	Nitration	1.95
Reduction	1.10	Halogenation	1.45	Pyrolysis	1.45
Alkylation	1.25	Hydrogenation	1.35	Electrolysis	1.20
Sulfonation	1.30	Polymerization	1.50	Aminolysis	1.40

- pn10 (type of undesirable side reaction):

Reaction type	pn10
Autocatalytic reaction	1.65
Non-autocatalytic reaction occurring at above normal reaction conditions	1.45
Non-autocatalytic reaction occurring at below normal reaction conditions	1.20

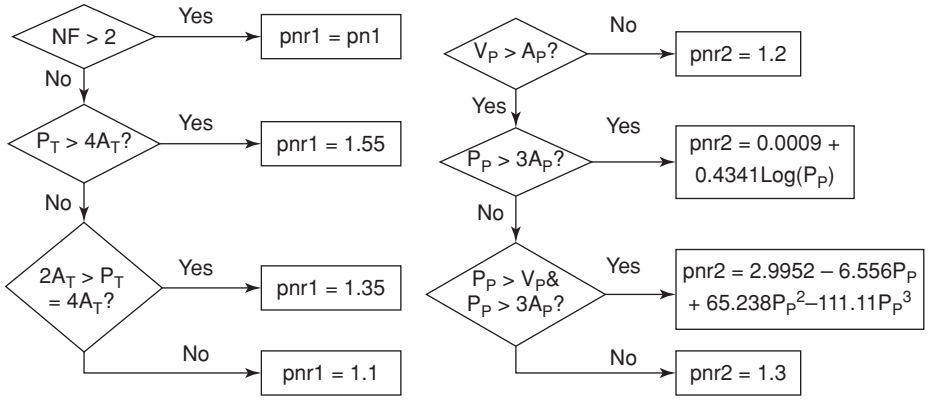

Figure 16.A2 *Calculation of pnr1 (left plot) and pnr2 (right plot) for TDR.*

A.2 Penalty Calculation for TDR (Khan *et al.*, 2001)

- pnr1 (effect of temperature):
  The pnr1 parameter can be calculated based on Figure 16.A2. Here, A_T—ambient temperature (°C), P_T—process temperature (°C), NF—NFPA flammability rating.
- pnr2 (effect of pressure):
  The parameter, pnr2 can be calculated based on Figure 16.A2. Equations in this flowchart are obtained based on graphs in Khan *et al.* (2001); pressure in these equations is in atm.
- pnr3 (vapor density):
  pnr3 = 1.2 × vapor density/air density for vapor; pnr3 = 1 for liquid release. Here, vapor density is evaluated at process conditions, whereas air density is evaluated at ambient conditions.
- pnr4 (toxicity of chemical):
  pnr4 = Maximum (1, 0.6NH)
- pnr5 (due to population density):
  pnr5 = Maximum (1, 0.1538 × population density in thousand persons per km^2)
- pnr6 and pnr7 (external factors and vulnerability of surroundings):
  pnr6 = pn7 and pnr7 = pn8; pn7 and pn8 are calculated in appendix A.

A.3 3-D Plots for Optimization of EES Objectives

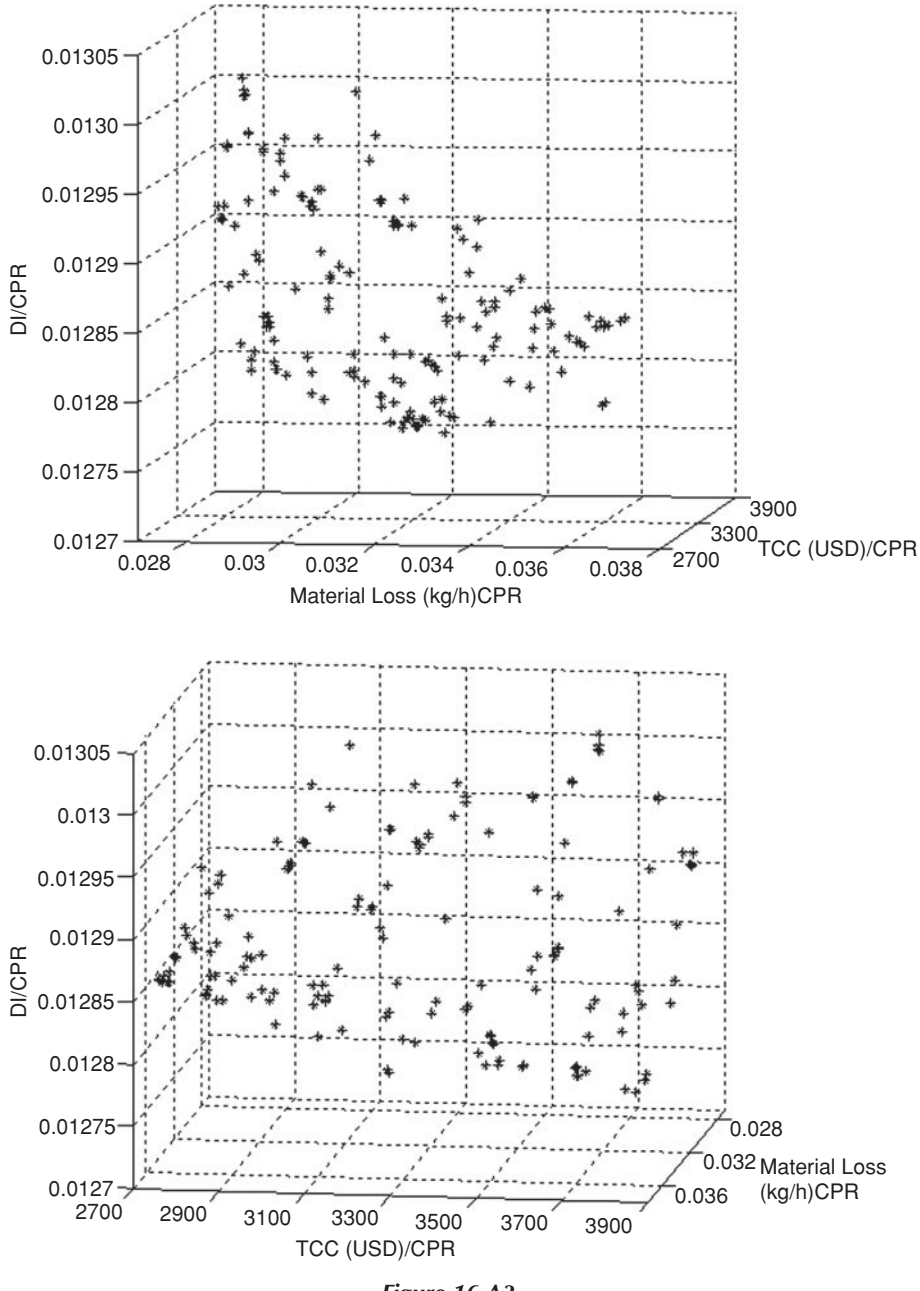

Figure 16.A3

References

Adu, I.K., Sugiyama, H., Fischer, U. and Hungerbühler, K. (2008), Comparison of methods for assessing environmental, health and safety (EHS) hazards in early phases of chemical process design, *Process Safety and Environmental Protection*, 86, 77–93.

Al-Sharrah, G., Edwards, D. and Hankinson, G. (2007), A new safety risk index for use in petrochemical planning, *Process Safety and Environmental Protection*, 85, 533–540.

Banimostafa, A., Papdokonstantakis, S. and Hungerbühler, K. (2012), Evaluation of EHS hazard and sustainability metrics during early process design stages using principal component analysis, *Process Safety and Environmental Protection*, 90(1), 8–26.

Deb, K., Pratap, A., Agarwal, S. and Meyarivan, T. (2002), A fast and elitist multi-objective genetic algorithm: NSGA-II, *IEEE Transactions on Evolutionary Computing*, 6, 182–197.

Edwards, D.W. and Lawrence, D. (1993). Assessing the inherent safety of chemical process routes: is there a relation between plant costs and inherent safety? *Chemical Engineering Research and Design*, 71(Part B), 252–258.

Gebreslassie, B.H., Guillen-Gosalbez, G., Jimenez, L. and Boer, D. (2009), Design of environmentally conscious absorption cooling system via multi-objective optimization and life cycle assessment. *Applied Energy*, 86, 1712–1722.

Guillen-Gosalbez, G., Caballero, J.A., Esteller, L.J. and Gadalla, M. (2007), Application of life cycle assessment to the structural optimization of process flow sheets. *Seventeenth European Symposium on Computer Aided Process Engineering*, 17, 163–1168.

Heikkilä, A.M., Markku, H. and Järveläinen, M. (1996), Safety considerations in process synthesis, *Computers and Chemical Engineering*, 20, S115–S120.

Hoffmann, V.H., McRae, G.J. and Hungerbühler, K. (2004), Methodology for early-stage technology assessment and decision making under uncertainty: application to the selection of chemical processes, *Industrial Engineering and Chemical Research*, 43, 4337–4349.

Khan, F.I. and Abbasi, S.A. (1998), Multivariate hazard identification and ranking system, *Process Safety Progress*, 17, 157–170.

Khan, F.I. and Amyotte, P.R. (2004), Integrated inherent safety index (I2SI): a tool for inherent safety evaluation, *Process Safety Progress*, 23, 136–148.

Khan, F.I. and Amyotte, P.R. (2005), I2SI: a comprehensive quantitative tool for inherent safety and cost evaluation, *Journal of Loss Prevention in the Process Industries*, 18, 310–326.

Khan, F.I., Husain, T. and Abbasi, S.A. (2001), Safety weighted hazard index (SWeHI): a new, user-friendly tool for swift yet comprehensive hazard identification and safety evaluation in chemical process industries, *Process Safety and Environmental Protection*, 79, 65–80.

Khan, F.I., Sadiq, R. and Amyotte, P.R. (2003), Evaluation of available indices for inherently safer design options, *Process Safety Progress*, 22, 83–97.

Khan, F.I., Sadiq, R. and Veitch, B. (2004). Life cycle index (LInX): a new indexing procedure for process and product design and decision-making, *Journal of Cleaner Production*, 12, 59–76.

Kidam, K., Hassim, M.H. and Hurme, M. (2008), Enhancement of inherent safety in chemical industry, Third International Conference on Safety and Environment in the Process Industry, Rome, Italy.

Lee, S.Q.E. and Rangaiah, G.P. (2009), Optimization of recovery processes for multiple economic and environmental objectives, *Industrial Engineering and Chemical Research*, 48, 7662–7681.

Lees, F.P. (2005), Lees' Loss Prevention in the Process Industries, 3rd edn., Elsevier.

Li, X., Zanwar, A., Jayswal, A., Lou, H.H. and Huang, Y. (2011), Incorporating exergy analysis and inherent safety analysis for sustainability assessment of bio-fuels, *Industrial Engineering and Chemical Research*, 50, 2981–2993.

Luyben, W.L. (2010), Design and control of the cumene process, *Industrial Engineering and Chemical Research*, 49, 719–734.

OSHAS 18000 and 18001 (n.d.), www.ohsas-18001-occupational-health-and-safety.com/ (accessed December 19, 2012).

Palaniappan, C., Srinivasan, R. and Tan, R. (2004), Selection of inherently safer process routes: a case study, *Chemical Engineering and Processing: Process Intensification*, 43, 641–647.

Ramzan, N. and Witt, W. (2006), Multi-objective optimization in distillation unit: a case study, *The Canadian Journal of Chemical Engineering*, 84, 604–613.

Seider, W.D., Seader, J.D., Lewin, D.R. and Widagdo. S. (2010), Product and Process Design Principles, 3rd edn., John Wiley & Sons, Inc.

Shah, N.M., Hoadley, A.F.A. and Rangaiah, G.P. (2009), Inherent safety analysis of a propane precooled gas-phase liquefied natural gas process, *Industrial Engineering and Chemical Research*, 48, 4917–4927.

Sharma, S., Chua, Y.C. and Rangaiah, G.P. (2011), Economic and environmental criteria and trade-offs for recovery processes, *Materials and Manufacturing Processes*, 26, 431–445.

Sharma, S., Rangaiah, G.P. and Cheah, K.S. (2011), Multi-objective optimization using MS Excel with an application to design of a falling-film evaporator system. *Food and Bioproducts Processing*, 90(2), 123–134.

Srinivasan, R. and Kraslawski, A. (2006), Application of the TRIZ creativity enhancement approach to design of inherently safer chemical processes, *Chemical Engineering and Processing*, 45, 507–514.

Srinivasan, R. and Nhan, N. T. (2008), A statistical approach for evaluating inherent benignness of chemical process routes in early design stage, *Process Safety and Environmental Protection*, 86, 163–174.

Suardin, J., Sammannan, M. and Elhalwagi, M. (2007), The integration of Dow's fire and explosion index (F&EI) into process design and optimization to achieve inherently safer design, *Journal of Loss Prevention in the Process Industries*, 20, 79–90.

Turton, R., Bailie, R.C., Whiting, W.B. and Shaeiwitz, J.A. (2003), Analysis, synthesis and design of chemical processes, 2nd edn., Prentice Hall.